

**FOCAL MECHANISM OF EARTHQUAKES
FROM THE JUNE 1987 SWARM IN ASWAN, EGYPT,
CALCULATED BY THE MOMENT TENSOR INVERSION**

Hassoup AWAD¹ and Grzegorz KWIATEK²

¹National Research Institute of Astronomy and Geophysics
11421-Helwan, Cairo, Egypt
e-mail: awad_hassoup@hotmail.com

²Institute of Geophysics, Polish Academy of Science
ul. Księcia Janusza 64, 01-452 Warszawa, Poland
e mail: gregus@igf.edu.pl

A b s t r a c t

We obtained seismic moment tensor solutions of ten events from the June 1987 earthquake swarm, which occurred along the Kalabsha fault zone in the northern part of the Lake Aswan area in Egypt. In addition, the composite fault plane solution of this sequence was also calculated. The waveform data were obtained from the Aswan seismological network, which consists of 13 field stations with short period seismometers GS-13. The June 1987 swarm was a sequence of microearthquakes ($M \leq 3.4$), shallow (0-10 km) events forming two successive bursts, which took place on June 17 and 19.

The moment tensor solutions indicate that the focal mechanisms of events from this swarm sequence are expressed by right-lateral strike slip faults. They represent also an effective east-west compressional stress field acting in the area. Geological and geophysical data demonstrate that the Kalabsha fault zone is a right-lateral strike slip fault that consists of several fault segments trending in the east-west direction, perpendicular to the axis of the main course of the Lake Aswan. Thus, the focal mechanisms of the 1987 events are consistent with the local tectonics of the area.

Key words: earthquake swarm, focal mechanism, moment tensor inversion, spectral ray-tracer, Lake Aswan.

1. INTRODUCTION

This study is carried out under the long-term scientific cooperation in seismology between the National Research Institute of Astronomy and Geophysics in Egypt and the Institute of Geophysics, Polish Academy of Sciences in Poland. The purpose of this study, which was suggested by Prof. Janusz Niewiadomski from the Institute of Geophysics in Warszawa, is to investigate in more details the seismotectonic picture of the focal region with earthquake swarm sequences in the Lake Aswan area. The digital waveform data were collected from the Aswan seismological network, which consists of 13 seismic short-period stations distributed in the northern part of Aswan Lake (Fig. 1). The seismic signals are transmitted from the field stations to a recording center located near the High Dam by radio-link (Awad, 1994; Simpson *et al.*, 1990).

The occurrence of swarm-type activity in the Aswan area is not frequent. There was only one remarkable swarm sequence, which occurred in June 1987 in the shallow part of the crust beneath the Wadi Kalabsha embayment, a westward extension from the Lake Aswan. This lake started to fill early in 1964 as a consequence of the High

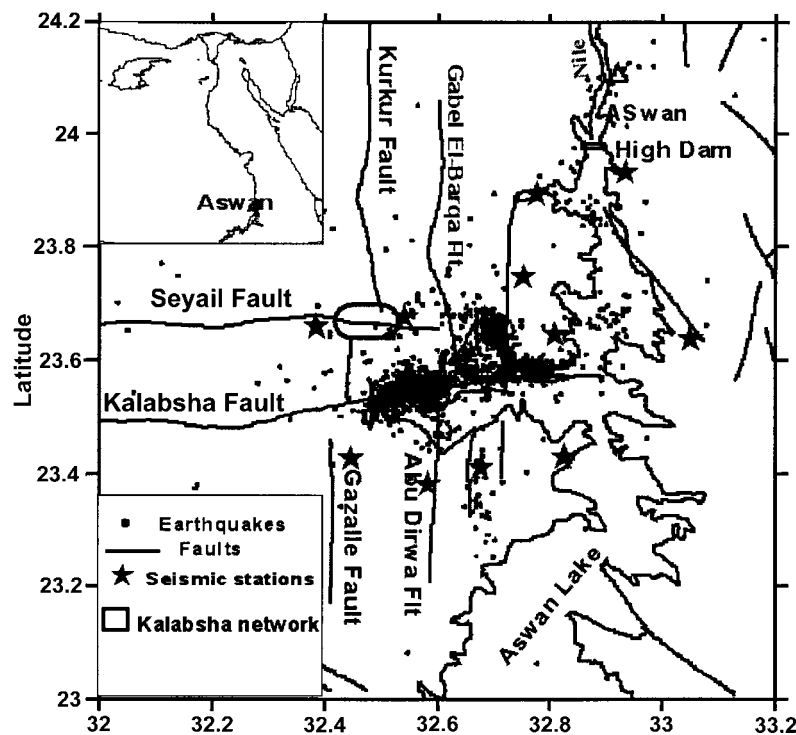


Fig. 1. Geological structure and seismicity of the Aswan Lake area (1981-2002).

Dam construction and now forms the second largest man-made reservoir in the world. It extends over 350 km along the Nile River in Egypt. On 14 November 1981, an earthquake of magnitude $M = 5.7$ occurred beneath the Lake Aswan and was related to the Lake Aswan reservoir impoundment (Kebeasy *et al.*, 1981). The Lake area is occupied by the Precambrian granite rocks that are uncomfortably overlain by a series of sedimentary units of age from the late Cretaceous to lower Eocene (Issawi, 1982). The major sedimentary unit in the area is the Nubian Sandstone, which covers generally the total area between the Lake Aswan on the east and Sin-Elkaddab plateau on the west. Many studies have been published describing the Aswan seismicity and its relation to the Lake (i.e., Kebeasy *et al.*, 1981; Awad, 1994; Awad and Mizoue, 1995a; Mekkawi *et al.*, 2002; 2004). Based on seismotectonic analyses, in particular a 3D crustal tomography study, Awad and Mizoue (1995b) separated this seismicity into two groups (deep and shallow). Shallow events have focal depths of less than 10 km. Deep events extend from 10 to 30 km. The local crustal model developed by Kebeasy *et al.* (1992) and modified by Awad and Mizoue (1995b) was used for the location. The focal mechanism solutions were obtained for the larger earthquakes located in and near Aswan (Kebeasy *et al.*, 1981; Awad, 1994; Hassib, 1990). The Kalabsha fault is the main source of seismicity in Aswan that is characterized by hypocenters distribution within the total crust thickness.

The focal mechanism solutions provide the fault plane parameters (i.e., strike, dip, rake, P and T axes and other characteristics of the focal region) of seismic events. In this study the analyses are carried out based on the composite fault plane solution and seismic moment tensor inversion in the time domain with software routinely used in Polish copper ore mines. Different methods have been developed for the inversion of seismic moment tensor at far-field distances. The study of seismic source at regional distances and the moment tensor inversion in particular meets with several difficulties. One is the site effect, but the main problem is the correct separation of the seismic source effects from the path effects on the seismogram. For events with foci at shallow depths and short epicentral distances, however, the problem may be simplified since first arrivals correspond to direct P and S waves that travel upwards directly from the focus to the station, without experiencing much interference from the crustal structure.

2. LOCAL GEOLOGY AND TECTONICS

In the northern part of the Lake Aswan area, between latitudes 23.40°-23.72°N and longitudes 32.53°-32.88°E, the tectonics is dominated by east-west and north-south fault systems, as well as a regional uplift (El-Shazly, 1977) (Fig. 1). The 1981 Aswan earthquake was located on the east-west Kalabsha fault (Kebeasy *et al.*, 1981; Awad, 1994). The Seyail fault is another east-west trend located 12 km north of the Kalabsha fault. The Kalabsha and Seyail faults are bounding a graben structure of low seismic velocity zone (Awad, 1994). The north-south fault system runs nearly parallel to the

Lake main course in the area. The topography is complicated by structural faults and also by the presence of alkali granites and syenite ring complex. The Nubian sandstone formation and sediments are about 500 m thick, forming a generally flat area of low relief varying from 150 to 350 m. The Quaternary formation is represented by the calcite and Nile deposits (Issawi, 1978; 1982). Igneous and metamorphic rocks are distributed in several localities in the area west of the lake Aswan and constitute the main geological formation on its eastern side. The east-west and north-south fault systems affect the sandstone beds of the Nubian plain by normal and strike-slip faults.

The Sin-El-Kaddab plateau is a limestone plateau, extending westward from the boundary of the Nubian plain. It is characterized by variable relief, which ranges from extensive flat areas to rugged areas with highly resistant rock hills and breeches (Issawi, 1982). Its escarpment is retreating westward in an irregular pattern that may be structurally influenced by east-west and north-south fault sets in the region. The average elevation of the plateau is approximately 350 meters. The lower portion of the Sin El-Kaddab escarpment is predominantly composed of easily eroded shale beds that are called Dakhla formation. The upper portion is composed of the hard, resistant limestone beds that are known as Kurkur formation. The steeples of the escarpments are a result of differential erosion of these lithologic units. Several east flowing wadies have incised the Nubian plain near the western margin of the plain, west of the Aswan High Dam. The largest set is known as Wadi Kalabsha and Wadi Kurkur (Fig. 1). Wadi Kalabsha covers an area of 3500 km and surrounds Gabel Marawa, which represents a relict of the retreated Sin El-Kaddab scarp (Issawi, 1978). The summit of the Gabel Marawa rises 251 m above sea level. The floor width of this Wadi Kalabsha varies from place to place. It is of 3 km in some locations. Its depth ranges from 175 to 225 meters.

The geologically well-identified fault trends in the area are as follows. (1) The **Kalabsha fault**: this fault crosses the Nubian plain along Gabel Marawa over 300 km distance and is dominated by a right-lateral slip. The base of Gabel Marawa is affected by the Kalabsha fault along which beds are steeply inclined. (2) The **Seyail fault**: it is extended sub-parallel to and approximately 12 km north of the Kalabsha fault. Its length is about 90 km associated with a right-lateral slip displacement. (3) The **Kurkur fault**: it is about 44 km long in the north-south direction and its northern end is very near to the Aswan High Dam. It is dominated by a left-lateral slip. This fault is associated with small folds and steeply dipping beds (Issawi, 1978). In some portions, this fault is clearly expressed by a contact between the Nubian formation on the east and quaternary alluvium on the west. (4) The **Khour El-Ramla fault**: this fault is another segment trending north-south, of 36 km length, and its northernmost part is located about 17 km southwest of the High Dam. The west face of this fault exhibits scarp in front of the Nubian plain with a left-lateral slip mechanism of displacement. (5) The **Gaszal Fault**: it is also a north-south trending structure located south of the Kalabsha fault. It extends for about 35 km and has been inferred as a left-slip fault. Direction of its down throw is toward the east. The amount of down throw increases

toward the south (Issawi 1978). Along this fault, minor folds are locally well developed. (6) The **Abu-Dirwa fault**: it is trending in the north-south direction and is located a few kilometers east of the Gaszal fault. It has a length of 15 km and has been inferred as a left-lateral slip fault (Issawi, 1978).

The regional uplift and fault systems affected the Aswan region (Issawi, 1978; 1982; El-Shazly, 1977). The late Cenozoic orogeny is observed in two areas in Egypt. In the Red Sea area, this fault system is dominated by normal faults similarly as in the western desert; while the mechanism in the Nubian plain and Sin El-Kaddab plateau is of strike-slip type. The Nubian formation and its overlying units have been gently tilted toward the west and northwest. The regional dip of these units is about 1° to 2° (El-Shazly, 1977). There are small faults superimposed on essentially flat-lying structures of the Nubian plain and Sin El-Kaddab plateau. Some of these faults are relatively long running over large distance of more than 300 km. The Nubian sandstone bed is locally folded in some locations into small anticlinal and synclinal folds, which were developed along the fault traces (Issawi, 1978). The Aswan granite of pink colour represents the basement rocks on the western side of the river Nile. The gravity data in the Aswan area delineate the regional trends (e.g., the subsurface structures of the fault area west of the lake). The crustal thickness in Aswan ranges from 34 to 30 km beneath the Precambrian rocks and the sedimentary structures, respectively (Kebeasy *et al.*, 1992).

3. THE JUNE 1987 SWARM

The Lake Aswan seismicity was concentrated at the intersection between the east-west and north-south fault systems since 1981 (Kebeasy *et al.*, 1981; Awad, 1994; 2002). The most active zone is located on the Kalabsha fault, which was the source of the November 14, 1981, main earthquake ($M = 5.7$) (Kebeasy *et al.*, 1981). After 1981 main shock, an extended sequence of microearthquakes characterizes the Lake Aswan seismicity. The correlation between temporal variations of this seismicity and changes in water level in the Lake Aswan was carried out in several studies (i.e., Kebeasy *et al.*, 1981; Awad, 1994; 2002; Awad and Mizoue, 1995a) (Fig. 2). The earthquake activity in that area decreased substantially and remained low during the period from October 1985 to June 1987 when an earthquake swarm occurred, composed of events of magnitude between 0.5 and 3.5 within a depth interval from 5 to 10 km along the Kalabsha fault zone (Fig. 3). Awad *et al.* (2003) relocated events of this sequence using the seismogram waveform analysis and obtained a more concentrated zone for the epicentral distribution. The duration of this sequence was just 6 days, from 15 to 20 June with a concentration of events on 17 and 19 June (Fig. 4). Monitoring of water level variation shows that there was a remarkable fluctuation in the daily water level variation in the lake during the time of the swarm (Fig. 3).

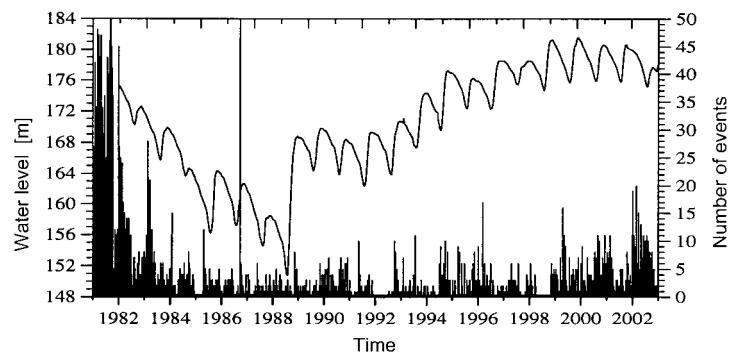


Fig. 2. Temporal variation seismicity and water level changes in the Lake Aswan area during the period from December 1981 to December 2002.

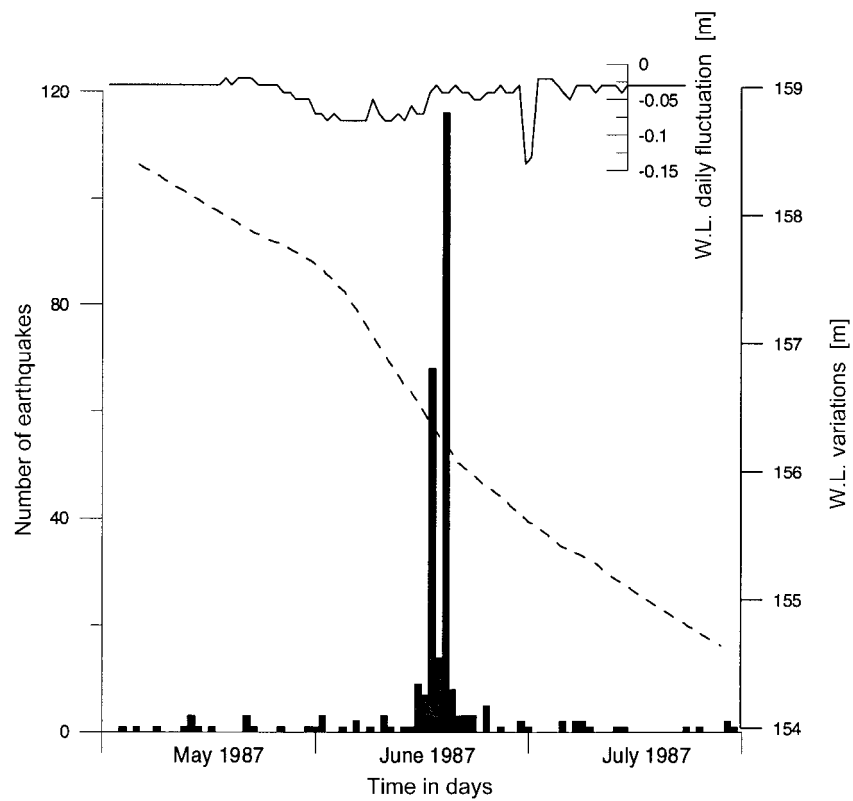


Fig. 3. Temporal variation of seismicity and water level (W.L.) and its daily fluctuation (calculated by subtracting the water level in each two successive days) in the Lake Aswan area, during the period from May to July 1987.

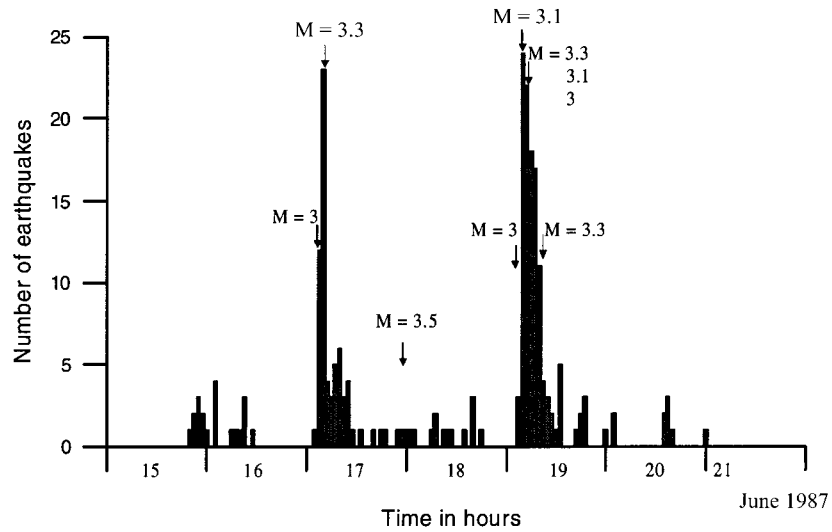


Fig. 4. Temporal distribution of the June 1987 earthquake swarm in the Lake Aswan area.

4. COMPOSITE FOCAL MECHANISM SOLUTION

The composite focal mechanism for earthquakes from the June 1987 swarm was calculated using the direction of the first *P*-wave motion on the Aswan seismic network records. These data are plotted on lower focal hemisphere using software developed by Suetsugu (1998). The field stations of this network are well distributed around the study area. The take-off angles were calculated using the local velocity model of the

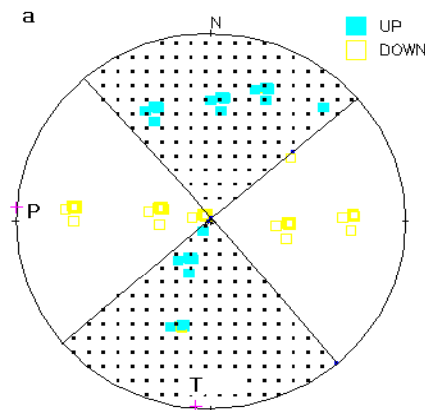


Fig. 5. The composite fault solution for the June 1987 Aswan earthquake swarm.

Table 1

Composite focal mechanism parameters

Nodal plane (1)			Nodal plane (2)			<i>P</i> -axis		<i>T</i> -axis	
strike	dip	rake	strike	dip	rake	plunge	trend	plunge	trend
229°	89°	179°	319°	89°	1°	0°	-86°	1°	184°

Aswan area as determined by Kebeasy *et al.* (1992). The composite focal mechanism shows a strike-slip fault with horizontal pressure and tensile axes (Fig. 5). Its parameters are listed in Table 1.

5. MOMENT TENSOR INVERSION USING SPECTRAL RAY-TRACER

The seismic moment tensor (SMT) is a general description of seismic point sources, establishing a linear relationship between the observed ground motion and a set of Green's functions or fundamental fault responses. Moment tensor inversion for small events in a geologically heterogeneous environment is not a trivial problem. The basic requirement for inversion is an appropriate set of waveforms, possibly with good azimuthal coverage, and including stations within a tectonically uniform travel-paths area. Also, the inversion procedure cannot be fully automated. A crucial manual task is refining the distance-dependent amplitude weighting until obtaining a stable inversion result and adequate waveform matches. This is generally an iterative procedure. Criteria to downweight or exclude waveforms are high noise level or propagation along complex paths (where Green's functions for plane layered media do not provide an appropriate correction). Traces may also be weighted to balance the station coverage over the focal sphere. Moment tensor estimates are usually sensitive to focal depth, and the linear moment tensor inversion with a grid search over a range of depths is usually combined to evaluate this non-linear effect. Once a moment tensor solution is obtained, it is double-checked by dislocation grid search modelling. This alternative way to invert double-couple focal mechanism serves as a resolution test: In this technique, waveforms for the full ranges of dislocation source orientations and depths are computed, and then compared with the observed seismograms to identify the range of valuable mechanisms. The fault-angle parameters: strike, dip and rake are sampled.

In the present study, inversion of the first *P*-wave amplitude of Aswan earthquake data is carried out using a method based on the work of Fitch *et al.* (1980) in order to calculate the moment tensor solutions. Only vertical component of the *P*-wave first arrival was taken into account. The recorded displacement for the vertical component of the *P*-wave phase is

$$U_z^p(x,t) = \frac{1}{4\pi\rho\alpha^3 r} \left[\bar{\gamma} M \dot{S} \left(t - \frac{r}{\alpha} \right) \bar{\gamma} \right] l_z, \quad (1)$$

where ρ is the average density, r is the source–receiver distance, α is the P -wave average velocity, M is the seismic moment, l_z is the cosine of the angle of incidence and $\bar{\gamma}$ is the take-off angle. Calculations of angles of incidence, take-off angles, average P -wave velocities and distances between stations and earthquakes were performed with a spectral ray tracer (Dębski and Ando, 2004), which is described in details later.

It is assumed here that the **Source Time Function** (STF) is based on Haskell’s source model (Haskell, 1953), and its derivative is of the form:

$$\dot{S}(t) = \begin{cases} 1/T & \text{for } 0 < t < T \\ 0 & \text{elsewhere} \end{cases} \quad (2)$$

where T is a rupture time.

This form of STF is expected to be a good approximation to the real mining -induced data (Wiejacz, 1991). Because the magnitude of analyzed events is similar to the magnitude of events recorded at Polish copper ore mines, the same form of STF has been chosen for selected earthquakes.

In order to calculate SMT, the following linear matrix equation was considered:

$$\mathbf{G}\mathbf{M} = \mathbf{U}_z^p, \quad (3)$$

where \mathbf{G} is a $N*6$ matrix (N is a number of recorded vertical amplitudes of e.g., the first P -wave velocity pulse). Matrix \mathbf{G} describes Green’s functions for the corresponding moment tensor elements, \mathbf{U} is a vector of the recorded displacements and \mathbf{M} is a vector containing 6 independent components of the SMT in the form:

$$\mathbf{M} = [M_{11}, M_{12}, M_{13}, M_{14}, M_{15}, M_{16}]. \quad (4)$$

Equation (3) is linear and, in common cases, when more than 6 independent values of the first amplitude of the P -wave phase are available, the solution can be obtained using any optimization procedure. The simplest solution is based on using L_2 norm (e.g., Wiejacz, 1991):

$$\sum_{i=1}^N (U_{z(i)}^p - G_{ij} M_j)^2 = \min. \quad (5)$$

However, a procedure that is more robust and less sensitive to large errors in data is based on using the L_1 norm (Claerbout and Muir, 1973):

$$\sum_{i=1}^N |U_{z(i)}^p - G_{ij} M_j| = \min. \quad (6)$$

In order to compute the SMT solution, L_1 norm was used whenever possible, because of the possibility of existence of mistakes in accurate picking of the first P -wave

arrival. In order to calculate the double-couple solution, some additional restrictions on the form of the seismic moment tensor matrix were assumed:

$$\text{tr}(\mathbf{M}) = 0, \quad (7)$$

$$\det(\mathbf{M}) = 0, \quad (8)$$

where $\text{tr}(\cdot)$ and $\det(\cdot)$ means the trace and the determinant of the moment tensor matrix. These restrictions lead to the inverse problem becoming nonlinear and it is advised to use, for example, the method of the Lagrange multipliers (Wiejacz, 1991) in solving eq. (6) according to constrains (7) and (8).

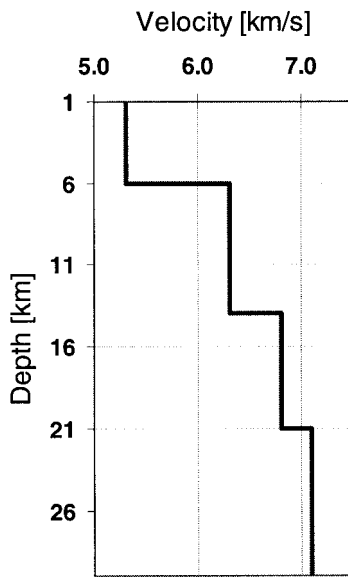


Fig. 6. 1D velocity model for the Aswan region used in the spectral ray-tracer.

In order to compute the angle of incidence, take-off angle, source–receiver distance, and average *P*-wave velocity for a particular source–receiver position, the spectral ray tracer (SRT) (Dębski and Ando, 2004) was used. SRT is a two-point ray-tracing algorithm based on the parameterization of ray paths by a series of Chebyshev polynomials. This pseudospectral approximation of sought ray paths allows reaching a very high accuracy of travel time calculations, and a simple calculation of the angle of incidence, take-off angle and the length of ray path between the source and receiver. SRT is a part of the larger software package, TOM3D (Dębski, 2002).

For the calculations we adopted a 1D velocity model for the Aswan region, which is shown in Fig. 6.

Firstly, the ray path was represented in parametric form with the coordinates $(l, 0, z)$, where l means the epicentral distance, and z means the difference between the depth of the source and station altitude. The ray path was described by two independent functions of ray parameter:

$$\mathbf{x}(\xi) = \begin{cases} l(\xi+1)/2 \\ z(\xi) \end{cases} \quad \text{for } -1 \leq \xi \leq 1 \quad (9)$$

and we assumed that $\mathbf{x}(-1) = \begin{pmatrix} 0 \\ z_0 \end{pmatrix}$ is the earthquake position at the depth of z_0 and

$\mathbf{x}(1) = \begin{pmatrix} l \\ h \end{pmatrix}$ is a station epicentral distance l and station altitude h , respectively.

In next step, the SRT algorithm discretizes the ray path described by eq. (9) and approximates it by the finite sum of the Chebyshev polynomials (Dębski and Ando, 2004):

$$z(\xi) = \sum_{i=0}^{N_z} a_i T_i(\xi), \quad (10)$$

where a_i are the expansion coefficients $T_i(\xi)$ is the Chebyshev polynomial of rank N .

In this study, the maximum rank of Chebyshev polynomials N was empirically assumed to be $N = 20$ as a compromise between the accuracy and speed of calculations. Finally, the travel time along the ray path is the line integral of slowness; in our 1D case, it is in the form:

$$T = \int_{-1}^1 s(\mathbf{x}(\xi)) \sqrt{1 + \left(\frac{dz(\xi)}{d\xi} \right)^2} d\xi, \quad (11)$$

where $s(\mathbf{x})$ is the slowness distribution according to the prepared 1D velocity model. A similar integral without the slowness term describes the length of the ray path l .

Representation of the ray paths in terms of a finite series of Chebyshev polynomials leads to the parameterization of the travel time function with finite number of decomposition coefficients $\{a_i\}$ (Dębski, 2002). Therefore, the optimization task of finding the shortest travel time path according to Fermat's principle, is the task of searching for the coefficients $\{a_i\}$, for which travel time T reaches the global minimum. This optimization task can be solved with any optimization algorithm. However, due to the nonlinearity of the problem, the best way to solve it accurately is to use any kind of the global optimization algorithm (Velis and Ulrych, 2001).

The SRT package allowed us to use a built-in global optimization algorithm based on the idea of Adaptive Simulated Annealing (ASA) (Ingber, 1989; 1993) to find the minimum travel time ray path for various depths and epicentral distances. We assumed the following annealing scheme: starting temperature equal to 100, final temperature was set to 10^{-14} with the total number of iterations of 60,000 and the maximum rank of Chebyshev polynomial equal to 20. For each earthquake depth and epicentral distance in our interest, the SRT was able to find the shortest ray path from the source to the receiver, thus we were able to calculate the angle of incidence, take-off angle, average P -wave velocity, and ray length.

Seismic moment tensor calculations were performed with Foci, the software routinely used in Polish copper ore mines¹ for mining-induced seismic events. The infer-

¹ Foci web page: <http://www.igf.edu.pl/~gregus/foci.php>

red focal mechanism solutions of the ten events from the June 1987 Aswan swarm are presented in Fig. 7. The lower-hemisphere, equal-area projection was used. Fault plane solution parameters are listed in Table 2 and the corresponding moment tensor components for double-couple solution are listed in Table 3. Moment magnitude M_w was calculated according to the standard relation given by Hanks and Kanamori (1979).

$$M_w = \frac{2}{3} \log M_0 - 6.0. \quad (12)$$

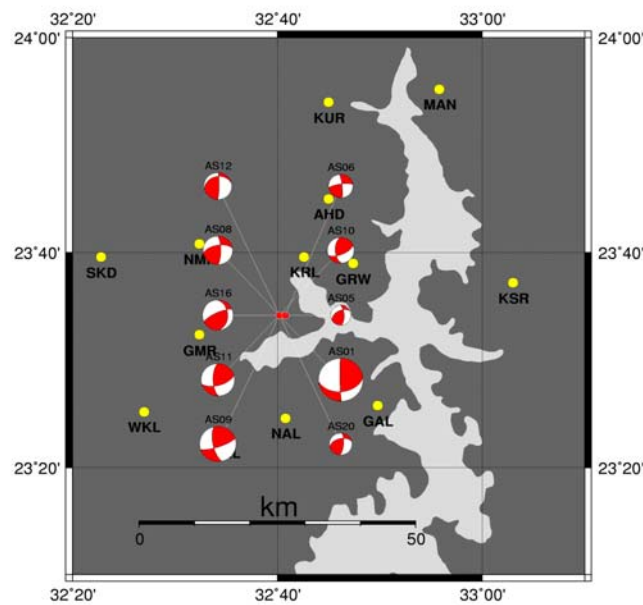


Fig. 7. Fault plane, double-couple solutions calculated for 10 selected events based on the seismic moment tensor inversion. The lower-hemisphere, equal-area projection is used. The size of a solution corresponds to the magnitude of the event (see Table 2 for details).

From Figs. 7 and 5 it follows that the moment tensor solutions are in reasonable agreement with the composite fault plane solution. The differences are caused mainly by a small number of the read first P -wave arrivals. The smallest number for the inversion procedure used by Foci is 8 to 10 of the first P -wave phases read (P. Wiejacz, personal communication). This requirement could be hardly fulfilled for some investigated events, especially for event AS05 (8 P -wave arrivals accurately picked) and

Table 2

Fault plane solutions obtained by the moment tensor inversion for selected events AS

Event no.	Date y m d	Time h m s	Lat. [deg]	Long. [deg]	Depth [km]	P-wave phases read	Fault plane A [deg]			Fault plane B [deg]			Seismic moment [N·m]	M_w
							trend	dip	rake	trend	dip	rake		
1	1987-06-19	9:07:16	23.57	32.67	6.9	12	179	86	47	85	43	133	9.38×10^{13}	3.3
5	1987-06-19	9:14:11	23.57	32.67	6.6	8	358	63	47	242	49	133	2.2×10^{11}	1.6
6	1987-06-19	10:13:14	23.57	32.68	9.5	13	354	82	14	262	76	166	5.95×10^{11}	1.9
8	1987-06-19	8:28:37	23.57	32.67	6.8	13	360	74	31	260	60	149	2.18×10^{12}	2.2
9	1987-06-19	8:29:20	23.57	32.67	6.9	15	72	77	23	167	68	157	1.29×10^{13}	2.7
10	1987-06-19	10:59:05	23.57	32.67	5.7	9	67	64	39	176	55	141	1.1×10^{12}	2
11	1987-06-19	12:54:50	23.57	32.67	6.8	13	179	66	32	74	61	148	5.85×10^{12}	2.5
12	1987-06-19	8:41:35	23.57	32.67	5.9	11	1	83	61	258	30	119	1.36×10^{12}	2.1
16	1987-06-19	8:01:32	23.57	32.67	6	11	246	75	57	358	36	123	2.97×10^{12}	2.3
20	1987-06-19	8:59:47	23.57	32.67	6.1	11	5	71	44	257	49	136	3.99×10^{11}	1.7

Table 3

Values of the six independent moment tensor components obtained by the moment tensor inversion for analyzed events AS

Event	Moment tensor components for double-couple solution						Maximum error
	T_{11}	T_{12}	T_{13}	T_{22}	T_{23}	T_{33}	
1	2.60×10^{12}	6.37×10^{13}	5.46×10^{12}	-1.13×10^{13}	6.79×10^{13}	8.71×10^{12}	3.35×10^{12}
5	8.74×10^9	1.28×10^{11}	-6.99×10^{10}	-1.39×10^{11}	-9.44×10^{10}	1.30×10^{11}	2.69×10^{10}
6	1.19×10^{11}	5.55×10^{11}	-9.64×10^{10}	-1.59×10^{11}	-1.28×10^{11}	4.05×10^{10}	2.55×10^{10}
8	3.11×10^{10}	1.79×10^{12}	-5.19×10^{11}	-6.26×10^{11}	-9.55×10^{11}	5.95×10^{11}	1.61×10^{11}
9	4.87×10^{12}	9.91×10^{12}	5.10×10^{12}	-7.13×10^{12}	1.20×10^{12}	2.26×10^{12}	1.07×10^{12}
10	9.72×10^{10}	7.28×10^{11}	5.47×10^{11}	-6.40×10^{11}	1.67×10^{11}	5.42×10^{11}	7.69×10^{10}
11	2.16×10^{11}	4.47×10^{12}	2.08×10^{12}	-2.53×10^{12}	2.01×10^{12}	2.31×10^{12}	3.03×10^{11}
12	-1.74×10^{10}	6.53×10^{11}	-6.8×10^{10}	-2.84×10^{11}	-1.16×10^{12}	3.02×10^{11}	6.64×10^{10}
16	1.19×10^{11}	1.51×10^{12}	-2.13×10^{12}	-1.40×10^{12}	4.93×10^{11}	1.28×10^{12}	1.47×10^{11}
20	-4.73×10^{10}	2.81×10^{11}	-7.55×10^{10}	-1.27×10^{11}	-2.25×10^{11}	1.74×10^{11}	2.94×10^{10}

AS10 (9 arrivals). For the others, the number of accurately picked first *P*-wave arrivals was between 11 and 15, and the solutions for these events should be more reliable.

6. DISCUSSION

The crustal deformation in Aswan area is controlled by the local tectonics and the presence of the Lake Aswan reservoir. In fact, earthquakes tend to be concentrated in space and time. Thus, investigations concerned with the relationship between the earthquakes and local tectonic characteristics are very important for further understanding of the earthquake-clustering phenomenon. This study is focused on the focal mechanism solutions, inferred from the moment tensor and composite fault plane analysis, to obtain a more detailed seismotectonic picture in the focal region of the earthquake swarm sequences. The earthquake swarms in Aswan are not frequent events. There has been only one typical swarm activity in that area since 1981. It occurred in June 1987 in the shallow part of the crust. The moment tensor solutions of ten events presented in this study from the June 1987 swarm consistently show strike-slip faulting and E-W oriented pressure axes that can be related directly to movements along fault segments of the Kalabsha fault zone. This small set of moment tensor solutions cannot be expected to sample adequately the tectonic deformation over the all area in Aswan, which is characterized by several geotectonic domains and complex neotectonic evolution (Issawi, 1978; 1982). The mechanisms presented here are generally similar to the focal mechanism of the November 14, 1981 main earthquake, expressed as a right-lateral strike-slip fault (i.e., Kebeasy *et al.*, 1981; Hassib, 1990; Awad, 1994). Geologically, the Kalabsha fault is also a right-lateral strike-slip fault. Thus, the focal mechanism solutions of the present study are consistent with the interpretation of local tectonics and results of the previous studies as observed above. Mekkawi (2003) studied the magnetotelluric and seismicity along active fault zones in the Aswan area and observed strike-slip faulting mechanism of these trends. There is no evidence suggesting heterogeneous tectonic stresses on a local scale. In other words, focal mechanisms of both large and small events in the Aswan area are quite similar.

The duration of the 1997 swarm was associated with fluctuations in daily water level variations in the Lake Aswan (Fig. 3). The simultaneous occurrence of the swarm and water level fluctuation is an important observation. Moreover, the events of the swarm were clustered in a narrow volume beneath the area covered by water (Wadi Kalabsha embayment) (Awad *et al.*, 2003) and were of low magnitude (Fig. 4). These are important features, which suggest that this activity was of different nature from the other events in the area. The Precambrian bedrock of the lake base is of poor permeability, however the water penetration through the base to the shallow depth of the crust is possible along faults and fractured zones. In addition, from a three-dimensional seismic velocity structural analysis, Awad (1994) and Awad and Mizoue

(1995b) have shown that the shallow part of the Kalabsha fault is characterized by a low seismic velocity anomaly. Furthermore, the Lake Aswan is the second largest artificial lake in the world and its load is different. Based on these observations, it seems proper to point out that the water penetration along the faulted and fractured Precambrian granite and its saturation in the Nubian sandstone cover increases the pore-pressure significantly.

The variation in patterns of the earthquake sequences is usually related to differences in the stress, pore pressure and material heterogeneity (Mogi, 1967; Wiemer and Benoît, 1996; Wiemer *et al.*, 1998). These conditions can provide important constraints for analysing the seismotectonic and hazard potential of a certain region (Malone and Wiemer, 2001). Generation of the June 1987 swarm may be partially correlated with the presence of the water reservoir due to its temporal variation pattern and the small magnitude of the events, which indicate their occurrence at a micro-fracture zone. The fluctuation of the water level in the Aswan lake as an independent observation suggests the possible penetration of the water across faults and fissures in a highly fractured shallow part of the crust and its associated influence on the stress regime, at least within the shallow crust. In addition, the presence of a low seismic velocity anomaly in the shallow part of the seismically active zone in the Lake Aswan area (Awad, 1994; Awad and Mizoue, 1995b) adds another factor, which would play an important role in studying the relationship between the seismicity parameters and the water reservoir-effective factors. The low seismic velocity anomaly is an environmental characteristic; it describes the instability of the active region where the medium deformation is often high either due to seismic or aseismic causes.

7. CONCLUSION

We applied the moment tensor inversion and composite fault plane techniques to obtain the focal mechanism solutions for ten events from the June 1987 swarm, which took place in the Lake Aswan area. The swarm-type earthquakes are not frequent in the Aswan area. Results of the present analyses and previous studies indicate a predominately strike slip-faulting regime in the northern part of the Lake Aswan area. We do not observe odd solutions, which would point to heterogeneity of faulting along the Kalabsha fault (main source of seismicity in the region). Effects induced by the Lake Aswan may occur at a shallow depth beneath the reservoir where the earthquakes of the June 1987 swarm were located. The pore pressure due to water penetration along cracks and fractures could be a very effective factor in the earthquake generation process, particularly in a region of low seismic velocity zone such as the shallow part of the Kalabsha fault. Thus, this study suggests that the earthquakes in the Lake Aswan area are mainly described by the tectonics and are occasionally affected by the presence of the Lake Aswan reservoir as well.

Acknowledgments. The first author is indebted to Professor Janusz Niewiadomski from the Institute of Geophysics, Polish Academy of Sciences in Warszawa, who left this life during the preparation of this work, for his help and organization of a visit to Warszawa. We are grateful to Professor Sławomir J. Gibowicz, for his help and encouragement during preparation of this work. We thank also the staff members of the Aswan Seismological Centre for providing the earthquake data from the Aswan area.

References

- Awad, H., 1994, *Investigation of the tectonic setting, seismic activity and crustal deformation in Aswan seismic region, Egypt*, Ph.D. Thesis, Tokyo University (unpublished).
- Awad, H., 2002, *Seismicity and water level variations in the Lake Aswan area in Egypt 1982-1997*, *J. Seism.* **6**, 459-467.
- Awad, H., and M. Mizoue, 1995a, *Earthquake activity in the Aswan region, Egypt*, *Pageoph* **145**, 1, 69-86.
- Awad, H., and M. Mizoue, 1995b, *Tomographic inversion for the three-dimensional structure of the Aswan region, Egypt*, *Pageoph* **145**, 1, 193-207.
- Awad, H., P. Denton, P. Maguire and G. Hassib, 2003, *Relocation of swarm events in the June 1987 earthquake sequence from the Lake Aswan area in Egypt*, *Pageoph* **160**, 1245-1257.
- Claerbout, E.W., and F. Muir, 1973, *Robust modeling with erratic data*, *Geophysics* **38**, 826-844.
- Dębski, W., 2002, *Seismic tomography software package*, *Publs. Inst. Geophys. Pol. Acad. Sc.* **B-30**, 103 pp.
- Dębski, W., and M. Ando, 2004, *Spectral ray tracer: A class of accurate two-point ray tracers*, *Acta Geophys. Pol.* **52**, 1-13.
- El-Shazly, E.M., 1977, *The geology of the Egyptian region*, *The Ocean Basin and Margins* **145**, 193-207.
- Fitch, T.J., W.D. McCovan and M.W. Shields, 1980, *Estimation of the seismic moment tensor from teleseismic body wave data with applications to intraplate and mantle earthquakes*, *J. Geophys. Res.* **85**, 3817-3828.
- Hanks, T.C., and H. Kanamori, 1979, *A moment magnitude scale*, *J. Geophys. Res.* **84**, 2348-2350.
- Haskell, N.A., 1953, *The dispersion of surface waves in multilayered media*, *Bull. Seism. Soc. Am.* **43**, 17-34.
- Hassib, G.H., 1990, *A study on the earthquake mechanics around the High Dam Lake, Aswan, Egypt*, Ph.D. Thesis, Faculty of Science, South Valley Univ., Sohag, Egypt (unpublished).

- Ingber, L., 1989, *Very fast simulated re-annealing: A comparison*, Oper. Res. Manage. Sci. **33**, 523.
- Ingber, L., 1993, *Simulated annealing: Practice versus theory*, Mathematical Computer Modelling **18**, 29-57.
- Issawi, B., 1978, *Geology of Nubia west area, western desert*, Ann. Geol. Survey Egypt.
- Issawi, B., 1982, *Geology of the southwestern desert of Egypt*, Ann. Geol. Survey Egypt.
- Kebeasy, R.M., M. Maamon and E.M. Ibrahim, 1981, *Aswan Lake induced earthquakes*, Bull. Intern. Inst. Seism. Earthq. Engin. **19**, 155-160.
- Kebeasy, R.M., A.I. Bayoumi and A.A. Gharib, 1992, *Crustal structure modeling for the northern part of the Aswan Lake area using seismic waves generated by explosions and local earthquakes*, J. Geodyn. **14**, 1-24.
- Malone, S., and S. Wiemer, 2001, *A software package to analyze seismicity: ZMAP*, Seism. Res. Lett. **72**, 374-383.
- Mekkawi, M., 2003, *Magnetotelluric and seismicity studies along active fault zones*, Ph.D. Thesis, Faculty of Science, University of Neuchatels, Switzerland (unpublished).
- Mekkawi, M., A. Hassoup, J.-R. Grasso and P.-A. Schnegg, 2002, *Fractal and spectral analysis of the earthquake sequences along Aswan Lake, Egypt*, EGS Nice, April, SE085.
- Mekkawi, M., J.-R. Grasso and P.-A. Schnegg, 2004, *A long-lasting relaxation of seismicity at Aswan, Egypt, 1982-2001*, Bull. Seism. Soc. Am. **94**, 479-492.
- Mogi, K., 1967, *Earthquakes and fractures*, Tectonophysics **5**, 35-55.
- Simpson, D.W., A.A. Gharib and R.M. Kebeasy, 1990, *Induced seismicity and changes in water level at Aswan reservoir, Egypt*, Gerlans. Beitr. Geophysik Leipzig **99**, 191-204.
- Suetsugu, D., 1998, *Practice on source mechanism*, IISSE Lecture Notes, 104 pp.
- Velis, D.R., and T.J. Ulrych, 2001, *Simulated annealing ray tracing in complex three-dimensional media*, Geophys. J. Int. **145**, 447-459.
- Wiejacz, P., 1991, *Investigation of focal mechanisms of mine tremors by the moment tensor inversion*, Ph.D. Thesis, Inst. Geophys. Pol. Acad. Sci., Warszawa (in Polish, unpublished).
- Wiemer, S., and J. Benoit, 1996, *Mapping the b-value anomaly at 100 km depth in the Alaska and New Zealand subduction zones*, Geophys. Res. Lett. **23**, 1557-1560.
- Wiemer, S., S. McNutt and M. Wyss, 1998, *Temporal and three dimensional spatial analysis of the frequency-magnitude distribution near Long Valley Caldera, California*, J. Geophys. Int. **134**, 409-421.

Received 1 March 2005
Accepted 22 March 2005